tech ops

TECHNICAL OPERATIONS RESEARCH

DASA-1800-II

DEPARTMENT OF DEFENSE
LAND FALLOUT PREDICTION SYSTEM

Volume II - Initial Conditions

TO-B 66-44

30 September 1966

Prepared By

H. G. Norment, W. Y. G. Ing, and J. Zuckerman
Technical Operations Research

This research has been sponsored by the
Defense Atomic Support Agency
under NWER Subtask A7a/10.058

Submitted to

U. S. Army Nuclear Defense Laboratory
Edgewood Arsenal, Maryland

Burlington, Massachusetts

For three REDWING shots — Tewa, Zuni, and Lacrosse — total soil masses in the clouds were obtained by analysis of specific activity data* that were measured from fallout samples collected for these shots. Specific activities for Ce^{144} were used instead of Mo^{99} data for reasons discussed in Section 4.9 of Ref. 20. Selected data recommended by Mr. R. C. Tompkins, Nuclear Defense Laboratory, from Tables 3.21, 3.24, and 3.25 of Ref. 20 were used. Specific activities, in units of fissions/unit mass of sample, for the remaining four shots were taken from Miller[21] (Table 3.11); these specific activities were based on Mo^{99} data.

For SUN BEAM Small Boy, radiological data as well as mass deposition data were obtained at the fallout collection stations. This afforded the opportunity to compare masses estimated by the two methods. If we exlude the results from two stations which appear to be spurious, the average mass determined by the specific activity method agrees with the value obtained by integration of the fallout mass deposition data to within 40%.

Major sources of error in the two methods of data reduction are known, but quantitative determinations of the errors are not possible since the total fallout from a nuclear explosion has never been determined. In the method of direct mass integration, the largest error lies in the assumption that the mass measured on the ground contains all the fallout, and thus all the soil mass in the cloud. A sizable proportion of the lightest particles in the cloud settle well beyond the range of the close-in fallout area. In fact, many particles are carried far aloft and contribute to worldwide fallout. This effect is particularly enhanced if the winds above the blast site are strong. Errors of this type are expected to be minimized for underground shots and shots in soil with relatively large soil particle sizes, since we then expect lower cloud heights and faster particle fall rates. A second major source of error is caused by contamination in the collectors. Since fallout areas are too hot to be entered immediately, ambient winds naturally will add dust to some collectors before the samples can be recovered. For SUN BEAM Small Boy, which was

*The specific activity method consists essentially of extrapolating measured specific activities to zero time, conversion from curies/mg of sample to equivalent fissions, and finally division into the total number of fissions produced by the detonation.

exploded over soil in the talc-size range, both sources of error may have seriously biased the observed size distributions. Although TEAPOT Ess was detonated in soil which had larger granules than SUN BEAM Small Boy, there was a base surge which extended out well over a mile from ground zero. The close-in stations therefore may have collected a significant amount of material that could not properly be classified as fallout.

The main source of error in determining soil mass loading of the cloud by activity measurements lies in determining an average value of the specific activity. Specific activity will vary with particle size and location. Since the number of collection stations for the tests for which this method was used were too few to accurately determine the average specific activity with respect to location, we were forced to assume that the measurements actually available were representative of the average specific activities.

Development of Scaling Functions. After the total fallout mass had been determined for the nine cases, two models, one for subsurface and the other for air bursts, were developed to correlate the results with yield and height of burst. We necessarily relied heavily on observed phenomenology associated with nuclear blasts. For surface and subsurface bursts we found it natural to ask whether mass lifted could be correlated with crater volume. We plotted fallout mass versus crater volumes as calculated for a paraboloid-shaped crater (from crater data given in Ref. 11). The graph shows that it is reasonable to suppose that a power-law relationship holds between the mass lifted and the volume of the resulting crater. The slope of the least squares straight line fitted to the data is 0.86. Since the plot is on a log-log scale, this slope implies that to the extent that our data are reliable, we may assert that the mass lifted in a detonation is approximately directly proportional to the volume of the crater produced.

The problem of the yield and depth of burst dependence of the soil loading is now much more tractable since we need look only at the dependence of crater volumes on yield and depth of burst, an area that has been investigated much more thoroughly than that of the fallout mass itself. Specifically, the relationship of crater volume to yield and depth of burst has been investigated in detail by Nordyke.[8] While the functions he derives are based only on high explosive bursts, his comparison of the

functions with data from low-yield nuclear bursts shows compatibility, the discrepancies in crater dimensions being no more than 10%. One obvious difficulty in calibrating a volume scaling function is the lack of really pertinent data at very high yields. Because of this, and since data on craters produced by high-yield explosions are in general sparse, we have chosen to use Nordyke's scaling functions extrapolated to the high-yield region. Nordyke's functions correlate quite well with the available crater data for the high-yield region. We have, then:

$$M = K_z R^2(z) D(z) W^{3/3.4} , \tag{10}$$

where

M = the total mass of soil in the cloud (g)

W = the yield (KT)

z = the scaled depth of burst ($ft \cdot KT^{-1/3.4}$)

$R(z) = 112.5 + 0.755z - 9.6 \times 10^{-6} z^3 - 9.11 \times 10^{-12} z^5$

$D(z) = 32.7 + 0.851z - 2.52 \times 10^{-5} z^3 + 1.78 \times 10^{-10} z^5$

and K_z is a constant (discussed later) that relates the crater volumes to soil mass lifted in the cloud.

For height of burst greater than zero, no study has been made of crater volumes comparable to that of Nordyke's for surface and subsurface bursts. Furthermore, crater-dimension data that are available do not correlate with yield in a consistent manner. Therefore, a different scaling model, based on the following rationalizations, was used for air bursts. The most intense blast and thermal effects of nuclear detonations are contained within the region of the fireball, and it is within the reach of this region that the cratering and soil incorporation take place. Of course, the dimensions of the fireball vary with time and never are precisely defined. However, we know that the fireball has a spherical shape, and we can reasonably assume that its volume is approximately proportional to the detonation yield. Therefore, a characteristic dimension of the fireball, for example the radius, will vary approximately as the cube root of the yield, namely

$r \sim W^{1/3}$. (This relation provides the basis for the form of the height of burst and depth of burst-scaling functions, $\lambda = hW^{-1/3}$ (Ref. 14, sections 3.55-3.58), or $\Lambda = hW^{-1/3.4}$ (Ref. 8).) If the cratering and soil incorporation occur within reach of the fireball, it is reasonable to expect that the mass of soil lifted will be proportional to the volume of the fireball segment that appears to be intersected by the ground (see Figure 7).

Figure 7. Intersection of a Fireball with the Ground

Our equation for estimating soil mass lifted by a nuclear cloud has the form of the equation for the volume of a segment of a sphere. This segment may be thought of as that portion of fireball volume that is intersected by the ground. In our equation the effects of yield and height of burst are expressed in the combined form of the scaled height of burst Λ. Figure 7 shows the pertinent geometry for a fireball with radius r and with its center at an altitude h above the ground. The hatched area represents the region of the fireball that intersects the ground, the volume of which is given by

$$V = \frac{\pi}{3}(r-h)^2(2r+h) \quad . \tag{11}$$

To specify a particular value for r, and at the same time provide a relationship between h and W that imposes a properly scaled limit on h above which no local fallout can occur, we note (Ref. 14, Section 2.118) that local fallout occurs only when the relation

$$h < 180W^{0.4} \tag{12}$$

is approximately obeyed. This relation provides us with an appropriate exponent to use on the yield in our scaling function; however, to be consistent and to ensure continuity at the ground surface between the scaling functions for subsurface and air bursts, we have chosen to continue to use $W^{1/3.4}$. Now, we define a radius-scaling function by

$$r = 180\, W^{1/3.4} \quad . \tag{13}$$

In terms of the scaled height of burst and radius-scaling functions, Eq. (13) becomes

$$V = \frac{\pi}{3} W^{3/3.4} (180 - \Lambda)^2 (360 + \Lambda) \quad . \tag{14}$$

Thus we obtain finally

$$M = K_\Lambda W^{3/3.4} (180 - \Lambda)^2 (360 + \Lambda) \quad . \tag{15}$$

The constants K_z of Eq. (10) and K_Λ of Eq. (15) were determined as follows. We noted that of all detonations studied, the mass data for TEAPOT Ess are by far the most reliable. Therefore, we used this single shot to calibrate the models. K_z was determined by direct solution of Eq. (10). Then, to satisfy the requirement of continuity at $z = \Lambda = 0$, we set Eqs. (10) and (15) equal and thereby obtained K_Λ. In light of the relative unreliability of the remainder of the observed data, this means of calibration is at least as valid as any other that might be proposed. Figure 8 shows calculated masses as a function of yield and height of burst.

The main justification for our models is the agreement between the calculated and the measured data. It is interesting to note that the Stanford Research Institute[22] experimentally determined that masses of soil lifted were proportional to crater volumes for a series of low-yield surface shots which they examined. They also determined that crater volume is proportional to yield to the 0.92 power which is in close agreement with our yield to the 3/3.4 = 0.88 power. Also, since the work reported here was completed, results of a somewhat similar study at the

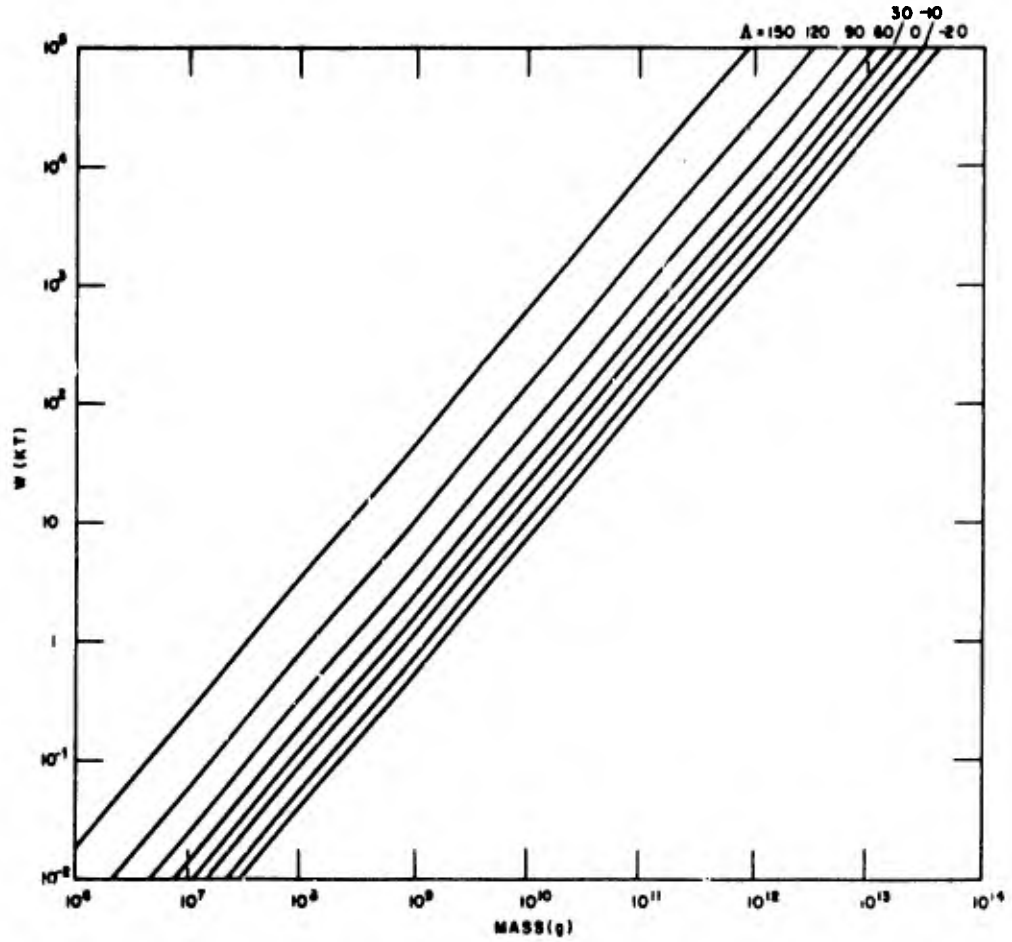

Figure 8. Calculated Total Soil Mass Lifted by the Cloud as a Function of Yield for Various Scaled Heights of Burst

Lawrence Radiation Laboratory have been released.[23] Total masses of soil material carried in clouds for a number of CASTLE and REDWING shots were determined by radiochemical analyses of samples collected by aircraft traverses through the clouds. For the four cases where these data can be compared directly with ours, mass ratio (ours/theirs) is 0.7 for the best case and 27 for the worst.

The complete set of equations governing the soil burden model are as follows:

$$M_{Soil} = K_z W^{3/3.4} R^2(z)\, D(z), \qquad 0 \leq z \leq 20$$

$$M_{Soil} = K_\Lambda W^{3/3.4} (180-\Lambda)^2 (360+\Lambda), \quad 180 \geq \Lambda \geq 0$$

where

M = the total mass of soil in the cloud (g)

W = the yield (KT)

Λ = scaled height of burst ($ft/KT^{1/3.4}$)

z = scaled depth of burst ($ft/KT^{1/3.4}$)

$R(z) = 112.5 + (7.55 \times 10^{-1})z - (9.6 \times 10^{-6})z^3 - (9.11 \times 10^{-12})z^5$

$D(z) = 32.7 + (8.51 \times 10^{-1})z - (2.52 \times 10^{-5})z^3 + (1.78 \times 10^{-10})z^5$

$K_\Lambda = 77.41\ g/ft^3$

$K_z = 2182\ g/ft^3$.

Phase Partitioning of the Soil Burden. In addition to the average cloud temperature and the total soil burden of the cloud, certain other information is essential to properly account for subsequent cloud rise and growth, distribution of activity among the particles, and the atmospheric transport of fallout. The thermodynamic cloud-rise computations must have the quantity of soil material in the vapor phase and the average temperature of condensed phase material. A knowledge of the fallout particle size-frequency distribution is essential to both the distribution of activity on the particles and atmospheric transport computations. To produce high quality estimates of the quantities mentioned would require an extensive combined theoretical and computational effort that would start from first principles and follow the many relevant complex processes from essentially shot time until the early cloud development. Such an effort never has been undertaken.

These particular problems are complicated by several considerations. At the time of interest, t_1, there is every reason to believe that a nuclear cloud has a grossly nonuniform structure with respect to soil content and temperature. Of particular significance is the sharp temperature gradient known to exist in the cloud. The cloud is very hot in the region of the ring through the cloud about which the toroidal circulation is centered. Beyond this region in all directions, temperature falls off rapidly with distance. One would expect to find essentially all of the radioactive device debris in the hot region of the cloud. Also, within this region one would expect to find whatever vaporized soil material is in the

cloud. As the cloud rises, this hot material continues to expand into its surroundings and, thereby, to heat and contaminate additional soil. In light of this description of the cloud structure it is apparent that actually it is inappropriate to use temperature and soil concentrations obtained by simple averaging over the total cloud volume. Also of importance here is the expectation that much of the soil burden in the hottest region of the cloud will not be in equilibrium contact with the hot gases there; in other words, we can expect a considerably lower average temperature to prevail for soil than for the gases in the cloud.

From Figure 1 it can be seen that immediately subsequent to t_1 the cloud begins to rise upward rapidly. A strong updraft is produced in the wake of the cloud, and soil dust suspended in air is sucked upward in the stem toward the cloud cap. The vortex circulation in the cloud[15, 16] is such as to cause very high upward circulation velocities to occur around the center axis of the cloud torus. This tends to pull some stem material into the bottom of the cloud and hence to incorporate this material into the outer cloud layers. This means that the cloud soil burden probably is incomplete at precisely t_1. We can expect, however, that the burden is completed very shortly thereafter. Unfortunately, there are not available quantitative data on internal cloud structure at times as late as those of interest here, nor do we know how much, if any, soil is incorporated into the cloud after t_1.

In the paragraphs that follow and in Appendix B, we present the results of tentative estimates for the fraction of the soil burden vaporized and the temperature of the condensed phase soil. This work was done after publication of our initial conditions final report[3] because additional information on cloud properties had become available, as mentioned earlier. Specifically, we have determined cloud altitudes and dimensions as a function of yield and height of burst at the initial time. This allows energy balance calculations to be made and we have applied these considerations to a determination of the desired quantities. We repeat that the information sought frequently is lost in the uncertainties that arise because of the approximations used to describe the energy partition model. The results are in a very real sense arbitrary, since by making different basic assumptions in the energy model, very different results can ensue. Furthermore, we must note

that of all possible plausible energy partition models, we have had the opportunity to investigate only one; fortunately this model does give physically reasonable results. Before proceeding into a discussion of the energy balance calculations let us consider some of the general properties of the system.

There are two categories of surface or soil material to be considered: siliceous and calcareous. Characteristic examples of siliceous soil are the common sandy and clay soils. In the case of sand, the chemical composition is almost pure silicon dioxide (SiO_2). For the much more abundant clays, the composition is more complex and there are significant quantities of a variety of metals such as aluminum and iron; but even for clays, the major chemical constituent is silicon dioxide. An average composition for igneous rock, from which the common clays are derived, is:[24]

Constituent	Percent Weight	Constituent	Percent Weight
SiO_2	60.18	CaO	5.17
Al_2O_3	15.61	Na_2O	3.91
Fe_2O_3	3.14	K_2O	3.19
FeO	3.88	TiO_2	1.06
MgO	3.56	P_2O_5	0.30

We see that the major constituents of clay soil (at high temperatures) are silica and alumina. Thermal properties for these materials are:[25,26]

Compound	Melting Temperature (°K)	Boiling Temperature (°K)
SiO_2	2000	3070
Al_2O_3	2323	3773

Common examples of calcareous surface materials are limestone and coral. These substances are essentially calcium carbonate ($CaCO_3$). However, at relatively low temperatures, calcium carbonate loses carbon dioxide gas to yield a

refractory residue of calcium oxide (CaO). Therefore, in considerations of calcareous material at high temperatures, we use the properties of calcium oxide; melting temperature 2853°K and boiling temperature 3123°K.[26]

We see then that the minimum boiling temperatures of siliceous and calcareous soils are approximately 3000°K and 3100°K, respectively. Figure 5 shows that cloud temperature at t_i sometimes is less than the boiling temperatures of the soil material. In such a case we simply take the fraction of soil in the vapor phase to be zero.

In estimating limits on the fraction of vapor phase soil for those cases where the cloud temperature is above that of the soil boiling temperature, we use the following realizations:

1. Temperatures in the cloud above the soil boiling temperature are localized to the region of the vortex ring core.
2. This (thermally) hot region of the cloud contains virtually all of the cloud radioactivity.
3. For surface bursts a large portion of fallout is derived from unvaporized soil particles on which radioactive weapon debris material condenses.
4. The amount of soil vapor in the cloud will be less than the mass of active fallout produced by the detonation.

We assert that item 4 follows from items 1, 2, and 3. At t_i the vaporized weapon debris material (which has a negligible total mass compared with the total soil burden mass) resides in the hot core ring of the cloud along with the vaporized soil. Both the debris material and the vaporized soil subsequently condense on solid or liquid soil particles to produce the radioactive portion of the cloud soil burden. Obviously the fallout material must include a significant amount of material that was never vaporized in addition to essentially all of the vaporized soil material. Therefore, the fraction of the total fallout mass that is found to be radioactive must exceed the fraction of vaporized soil in the cloud.

A survey of the literature to determine mass percent of active material observed in fallout has revealed that most of the mass and most of the activity are associated with particles in the large particle size range of the size-frequency distribution. For this reason, and since on the average there is only a slight tendency for specific activity of gross fallout to change with particle size, we shall concentrate our attention here on the larger particles. Table 1 is a summary of the best data available for large particles. We see that an average of approximately 50% of gross fallout mass is associated with active material. Therefore, on the basis of the reasoning presented above, we can state with a reasonable degree of confidence that, on the average, less than 50% of the total soil burden is vaporized.

TABLE 1

SELECTED MASS AND ACTIVITY DATA FOR LARGE PARTICLES

Operation / Shot	Particle Diameter Range (μ)	Approx. Mass of Total Fallout in Size Range (%)	Approx. Mass of Total Fallout Associated with Active Material in Size Range (%)	Source of Data
REDWING Zuni	> 420	75	75	Ref. 20 Fig. 3.53-3.55 Table 3.17
REDWING Tewa	> 210	90	75	Ref. 20 Fig. 3.57-3.59 Table 3.19
JANGLE Uncle	> 210	—	15	Ref. 22 Table IV (Station E)
SUN BEAM Small Boy	200-1000	58	27	Ref. 27 Table 8.2*
SUN BEAM Johnie Boy	> 200	80	50	Ref. 28 Table 3.17
AVERAGES		76	48	

*Only data from collection stations in the heavy fallout area were considered. These were stations 305, 405, and 503.

To be able to determine a more definite value for the fraction of the soil burden vaporized, and at the same time estimate the temperature of the condensed phase material, we have employed an energy partition analysis of the detonation. The critical problem in our analysis is to determine the fraction of the total detonation energy release that is consumed in heating and vaporizing soil. Since we already have relatively accurate knowledge of cloud altitude (therefore, pressure), cloud volume, temperature of the cloud gas, and total soil burden, a knowledge of energy available for heating and vaporizing soil allows estimates of the temperatures of the cloud contents to be made (see commentary on pp. 8 - 9).

Estimates of energies available for heating soil* were obtained by differencing the thermal energies radiated by air and surface bursts.[29] In Ref. 29 the thermal energy radiated is given as a function of yield for both air and surface bursts. With this maximum amount of energy available, it is a relatively simple matter to determine the desired quantities so that energy is conserved. The details are given in Appendix B. The results obtained are as follows:

1. 1.5% of the soil burden is vaporized per 100° excess of the initial temperature (as calculated from Eqs. (6), (7), and (8) over 3000°K for siliceous soils and 3100°K for calcareous soils.

2. The temperature ($^{\circ}$K) of the unvaporized soil is given by

$$T = 50 \log_{10} W + 1400$$

where W is the detonation energy yield in kilotons.

Particle Size Frequency Distribution

The problem of determining particle size-frequency distributions at t_1 is essentially the problem of determining the extent to which the preshot soil size-frequency distribution has been altered by the processes of evaporation and growth. In these considerations we can make a broad distinction between the high-yield and low-yield shots. We will consider high-yield shots first. At times prior to t_1, the fireball is extremely hot (see Figure 5) and because of the stable nature of the vortex circulation, which during the early stages of the cloud development tends to

*There may exist other means for estimating the available energy that are at least as plausible and can give different results.

insure that circulating material will remain contained within a limited region of the cloud, we can expect residence times of entrained material in the hot core to be long enough so that virtually all of this material will be completely vaporized. Beyond this region, condensed phase material should have essentially the preshot soil size-frequency distribution. Subsequent to t_1, additional soil may be entrained into the cloud; of course this also will have the preshot soil size-frequency distribution. Subsequent to t_1 we can expect growth to occur mainly by two mechanisms: (1) by condensation of vapor onto soil particles, and (2) by agglomeration of melted or partially melted soil particles. For high-yield shots we can expect both of these mechanisms to yield significant growth. The condensed phase material present as early as t_1, however, would be expected to have essentially the preshot soil size-frequency distribution.

For small detonations we note from Figure 5 that the "average" temperature at t_1 is below the boiling temperature of the soil material. We must assume, therefore, that there is essentially no soil vapor present at t_1. Also we note from Figure 3 that for the small detonations, t_1 is small; in other words, the time scale of events is greatly compressed for small detonations. This means that there is much less time available for thermal equilibrium between soil and cloud gases to be reached. We hypothesize, and this is supported by energy conservation calculations, that relatively little soil is ever vaporized in small detonations; consequently, there cannot have been significant particle growth by condensation from the vapor. Furthermore, since growth by agglomeration is a slow process, and the cloud cooling rate is very fast in relation to it (as shown by cloud rise simulation calculations), we conclude in light of the compressed time scale that growth by this mechanism also is not significant.

In summary, we find that the preshot soil size-frequency distribution is an adequate approximation to the size-frequency distribution of condensed phase material in the cloud at t_1. As a corollary to this finding, we anticipate that substantial particle growth occurs only for large-yield detonations.

REFERENCES

1. I.O. Huebsch, "The Development of a Water-Surface-Burst Fallout Model: The Rise and Expansion of the Atomic Cloud," USNRDL-TR-741 (23 April 1964).

2. I.O. Huebsch, "Development of a Land Surface Burst Cloud Rise Model," USNRDL-LR-145 (1965). (To be superseded by a USNRDL-TR)

3. H.G. Norment, W.Y.G. Ing, and J. Zuckermen, "Initial Conditions in the Nuclear Cloud," Technical Operations Research, Burlington, Mass., TO-B 65-118, AD369604L(February 1966). Secret-F.R.D.

4. H.G. Norment and S. Woolf, "Studies of Nuclear Cloud Rise and Growth Data," Proceedings of the Joint DASA-OCD Fallout Symposium," Monterey, California (12-14 April 1966). Secret-F.R.D.

5. H.G. Norment and S. Woolf, "Studies of Nuclear Cloud Rise and Growth," Technical Operations Research, Burlington, Mass., TO-B 66-9 (to be published). Secret-F.R.D.

6. Unpublished document on Cloud Characteristics, Edgerton, Germeshausen and Grier Report No. ET-833, prepared on contract AT(29-1) 1183. Secret-F.R.D.

7. R.W. Hillendahl, "Characteristics of the Thermal Radiation from Nuclear Detonations (U)," Vol. III, Naval Radiological Defense Laboratory, NRDL-TR-383 (30 June 1959). Secret-RD.

8. M.D. Nordyke, "On Cratering: A Brief History, Analysis, and Theory of Cratering," Lawrence Radiation Laboratory, UCRL-6578 (22 August 1961).

9. R.L. Stetson et al., "Distribution and Intensity of Fallout from the Underground Shot," Operation TEAPOT - Project 2.5.2, Naval Radiological Defense Laboratory, WT-1154 (14 March 1958).

10. P.D. LaRiviere et al., "Fallout Collection and Gross Sample Analysis (U)," Operation SUN BEAM, Shot Small Boy, Project 2.9, Naval Radiological Defense Laboratory, POR-2215 (October 1964). Secret-RD.

11. M. Morgenthau et al., "Compilation of Fallout Patterns and Test Data. Vol. II. Local Fallout from Nuclear Test Detonations," Nuclear Defense Laboratory, NDL-TR-34, DASA 1251 (August 1963). Secret-RD.

12. R. M. Davies and G. I. Taylor, "The Mechanics of Large Bubbles Rising Through Extended Liquids and Through Liquids in Tubes," Proc. Roy. Soc. A200, 375 (1950).

13. G. K. Batchelor, "Heat Convection and Buoyancy Effects in Fluids," Quarterly J. Roy. Meteor. Soc. 80, 339 (1954).

14. S. Glasstone, editor, "The Effects of Nuclear Weapons" (Washington, D. C.: USAEC, 1962).

15. H. G. Norment, "Research on Circulation in Nuclear Clouds," Technical Operations, Incorporated, TO-B 63-102 (1 December 1963).

16. H. G. Norment, "Research on Circulation in Nuclear Clouds, II (U)," Technical Operations, Incorporated, TO-B 64-102 (1 November 1964). Confidential-F. R. D.

17. J. F. Moulton, Jr., "Nuclear Weapons Blast Phenomena," U. S. Naval Ordnance Laboratory, DASA-1200 (March 1960). Section 1.5. Secret-RD.

18. B. Alder, S. Fernbach, and M. Rolenbert, editors, Methods in Computational Physics, Vol. 3, Fundamental Methods in Hydrodynamics (New York, N. Y.: Academic Press, 1964).

19. K. Steward, "The Condensation of a Vapor to an Assembly of Droplets of Particles (with Particular Reference to Atomic Explosion Debris)," Trans. Fara. Soc. 52, 161 (1956).

20. M. Morgenthau et al., "Land Fallout Studies (U)," Operation REDWING - Project 2.65, Chemical Warfare Laboratories, WT-1319 (1 February 1960). Secret-RD.

21. C. F. Miller, "Fallout and Radiological Countermeasures," Vol. I, Stanford Research Institute, SRI Project No. IM-4021 (January 1963). Chapter 3.

22. R. D. Cadle, "The Effects of Soil, Yield, and Scaled Depth on Contamination from Atomic Bombs," Stanford Research Institute, Project No. Cu-640 (29 June 1953). Secret-RD.

23. R. G. Gutmacher and G. H. Higgins, "Total Mass and Concentration of Particles in Dust Clouds (U)," UCRL-14397 (28 September 1965). Secret-RD.

24. B. Mason, "Principles of Geochemistry" (New York, N. Y. : John Wiley & Sons, 1952), p. 38ff.

25. H. L. Shick, "A Thermodynamic Analysis of the High Temperature Vaporization Properties of Silica," Chem. Rev. 60, 331 (1960).

26. C. D. Hodgman, editor, "Handbook of Chemistry and Physics," 44th Edition, The Chemical Rubber Publishing Co., Cleveland (1962).

27. E. C. Freiling, L. R. Bunney, and F. K. Kawahara, "Physico-chemical and Radiochemical Analysis (U)," Operation SUN BEAM, Shot Small Boy, Project 2.10, POR-2216, Naval Radiological Defense Laboratory (15 October 1964).

28. D. E. Clark, F. K. Kawahara, and W. C. Cobbin, "Fallout Sampling and Analysis: Radiation Dose Rate and History at 16 Locations (U)." Operation SUN BEAM, Shot Johnie Boy, Project 2.9, POR-2289, Naval Radiological Defense Laboratory (12 October 1963). Secret-RD.

29. "Capabilities of Atomic Weapons," Department of the Army Technical Manual, TM 23-200 (June 1955). Secret-RD.